Accepted Manuscript

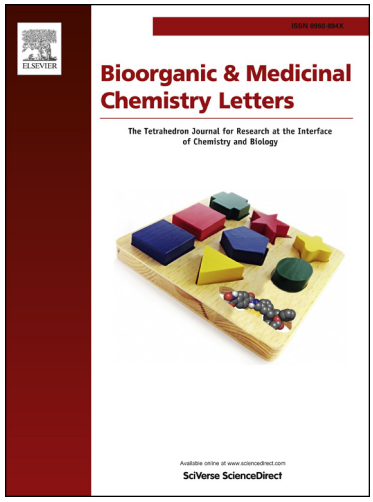

Imidazole - Derived Agonists for the Neurotensin 1 Receptor

Paul M. Hershberger, Michael P. Hedrick, Satyamaheshwar Peddibhotla, Arianna Mangravita-Novo, Palak Gosalia, Yujie Li, Wilson Gray, Michael Vicchiarelli, Layton H. Smith, Thomas D.Y. Chung, James B. Thomas, Marc G. Caron, Anthony B. Pinkerton, Lawrence S. Barak, Gregory P. Roth

PII: S0960-894X(13)01305-X
DOI: http://dx.doi.org/10.1016/j.bmcl.2013.11.026
Reference: BMCL 21053

To appear in: *Bioorganic & Medicinal Chemistry Letters*

Received Date: 2 October 2013
Revised Date: 6 November 2013
Accepted Date: 11 November 2013

Please cite this article as: Hershberger, P.M., Hedrick, M.P., Peddibhotla, S., Mangravita-Novo, A., Gosalia, P., Li, Y., Gray, W., Vicchiarelli, M., Smith, L.H., Chung, T.D.Y., Thomas, J.B., Caron, M.G., Pinkerton, A.B., Barak, L.S., Roth, G.P., Imidazole - Derived Agonists for the Neurotensin 1 Receptor, *Bioorganic & Medicinal Chemistry Letters* (2013), doi: http://dx.doi.org/10.1016/j.bmcl.2013.11.026

Imidazole - Derived Agonists for the Neurotensin 1 Receptor

Paul M. Hershberger*,[a], Michael P. Hedrick[b], Satyamaheshwar Peddibhotla[a], Arianna Mangravita-Novo[a], Palak Gosalia, Yujie Li, Wilson Gray, Michael Vicchiarelli[a], Layton H. Smith[a], Thomas D.Y. Chung[b], James B. Thomas[d], Marc G. Caron[c], Anthony B. Pinkerton[b], Lawrence S. Barak[c], Gregory P. Roth[a]

[a]*Conrad Prebys Center for Chemical Genomics at Sanford-Burnham Medical Research Institute, Orlando, Florida 32827, USA,* [b]*Conrad Prebys Center for Chemical Genomics at Sanford-Burnham Medical Research Institute, La Jolla, California 92037, USA and* [c]*Duke University Medical Center, Durham, NC 27710, USA*, *RTI International, 3040 E Cornwallis Road, Durham, North Carolina 27709, United States.*

This is where the receipt/accepted dates will go; Received Month XX, 2012; Accepted Month XX, 2013 [BMCL RECEIPT]

Abstract— A scaffold-hop program seeking full agonists of the neurotensin-1 (NTR1) receptor identified the probe molecule **ML301** (**1**) and associated analogs, including its naphthyl analog (**14**) which exhibited similar properties. Compound **1** showed full agonist behavior (79 - 93%) with an EC_{50} of 2.0 – 4.1 μM against NTR1. Compound **1** also showed good activity in a Ca mobilization FLIPR assay (93% efficacy at 298 nM), consistent with it functioning via the G_q coupled pathway, and good selectivity relative to NTR2 and GPR35. In further profiling, **1** showed low potential for promiscuity and good overall pharmacological data. This report describes the discovery, synthesis, and SAR of **1** and associated analogs. Initial *in vitro* pharmacologic characterization is also presented.

*To whom correspondence should be addressed. Tel. +1-407-745-2000. E-mail: phershberger@sanfordburnham.org

Methamphetamine addiction remains a substantial public health issue[1], and currently no small molecule therapies are available for its treatment. The tridecapeptide neurotensin[2] (NT) has neurological function known to influence reward behavior.[3-6] Neurotensin receptor 1 (NTR1) peptide agonists produce behaviors that are exactly opposite of the psychostimulant effects observed with methamphetamine abuse, such as hyperactivity, neurotoxicity, psychotic episodes, and cognitive deficits, and repeated administrations of NTR1 agonists do not lead to the development of tolerance[7,8]. Recent data from the Hanson laboratory[9] suggesting that NT receptor agonists may have a role in addiction therapy are: (a) in a methamphetamine self-administration rat model the substitution of the peptide NT agonist (Lys(CH_2NH)lys-Pro,Trp-*tert*-Leu-Leu-Oet) for methamphetamine did not significantly affect motor activity but dramatically reduced lever pressing (b) the peptide agonist was not self-administered, and (c) the effects were associated with nucleus accumbens dopamine D1 receptors. These findings strengthen the hypothesis that neurotensin receptors are valid targets for antagonizing drug seeking behaviors and preventing relapses. Although NTR1 has been known for many years, there have been few reports of relevant non-peptide ligands. A review of the isolation, cloning, localization, and binding properties of the accepted receptor subtypes (NTR1, NTR2, and NTR3) and the molecules known to bind at these receptors was published in 2009[10]. Also in 2009, the partial agonists **II-a, II-b,** and **II-c** (**Table 1**), structural analogs of the potent NTR1 antagonists SR48692 (**I-a**) and SR142948 (**I-b**), were identified using a Ca mobilization FLIPR assay[11,12]. Replacement of the adamantyl group in **I-a** with a panel of amino acid derived substituents revealed that the isobutyl group derived from L-leucine gave the best results. Eliminating one of the methoxy groups in **II-a** reduced the potency but improved efficacy (**II-c**). Researchers at Wyeth reported two different chemotypes, **III** and **IV**, each of which showed partial agonist activity for NTR1 in the FLIPR assay[13].

Table 1. Chemical Structures of Previously Reported Small Molecule NTR1 Agonists and Antagonists.

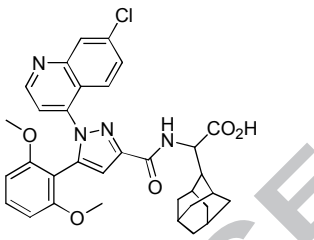

I-a (SR48692)

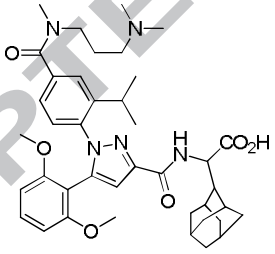

I-b (SR142948A)

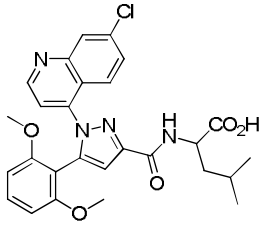

II-a, from L-leucine
II-b, from D-leucine

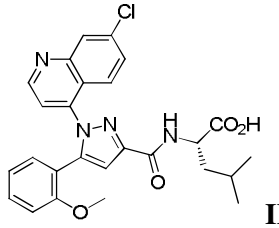

II-c

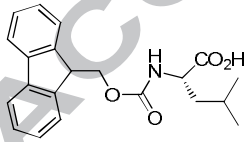

III, Fmoc-leucine

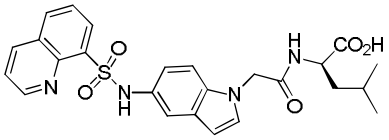

IV

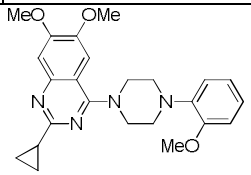

ML314

This project sought novel and improved small molecule neurotensin receptor agonists using a primary assay based upon the ability of a β-arrestin fluorescent reporter to directly recognize the activated state of NTR1. We recently reported[14] the discovery of the quinazoline **ML314** (**Table 1**), a nonpeptidic β-arrestin biased agonist, which resulted from a screening program using the NIH Molecular Libraries Small Molecules Repository (MLSMR) of >300,000 compounds followed by medicinal chemistry driven SAR studies.

In parallel, a scaffold-hop program was conceived from our evaluation of existing literature (**Table 1**). As assays were already being developed for the screening program, the opportunity to examine scaffold-hop molecules was an

attractive way to extend our work to chemotypes not present in the MLSMR. This led to the identification of the imidazole-based agonist **ML301** and associated analogs described herein.

The new compounds were synthesized according to the two routes outlined in **Scheme 1**. Although the alternate method was fewer steps, its low yields and the high cost of 4-aminoquinoline building blocks made the longer method more preferred and practical for most cases of interest. In addition to standard Pinner conditions, which generally do not work well for cases involving sterically hindered benzonitriles, many amidine-forming conditions were attempted[15-20] for the generation of **G**. Conditions (h), although inefficient, were the best we found for this sterically and electronically disfavorable case. For some analogs without the 2,6-dimethoxy moiety, the shorter route was more preferred. Importantly, both routes produced exclusively the key intermediate regioisomer **D** shown in the box, and there is ample literature precedent[15,21-23] for this assignment via the amidine (alternate) route. While it may appear that the preferred route could be shortened by performing the N-arylation step on the trifluoromethyl intermediate followed by CF_3 hydrolysis and amino acid coupling, this was not possible because the CF_3 hydrolysis failed if the imidazole was N-arylated, and the N-arylation was not efficient when performed on the acid intermediate. Thus, it was necessary to first hydrolyze the CF_3 group (b), and then esterify (c) prior to N-arylation (d).

Overall, variation at the R^1 and R^2 positions was emphasized, as a survey of R^3 groups for the pyrazole scaffold was already disclosed[11]. **Table 2** shows that R^1 is preferably both electron donating and sterically demanding; hence, the preference for 2,6-dimethoxy (**1**, **2**, **5**, **14**). A large loss of activity was observed when electronics were maintained but the steric factor was reduced via the 2,4-dimethoxy case (**11**). When the steric factor was maintained but the electron donating effect was either changed to electron withdrawing via the 2,6-dichloro case (**12**) or lowered via the 2,6-dimethyl case (**13**), agonism was maintained but the potency fell by 2.6x (**12**) and 4.6x (**13**). Other examples with lesser steric and / or electronic factors at the R^1 position were also much less active; namely, the 2-methoxy case (**3**) and the unsubstituted case of R^1 = H (**4**). The R^2 position accommodated 7-chloroquinoline (**1**), 7-H-quinoline (**5**), and 1-naphthyl (**14**) motifs. Generally, compounds bearing the 7-Cl group were better than the corresponding 7-H cases (**1**, **3**, and **4** versus **5**-**7**). For example, the 7-Cl compounds were more efficacious and, both **4** and **5** retained low potency whereas **6** and **7** were completely inactive. When the bicyclic aryl system at R^2 was replaced by either a 4-pyridyl (**8**-**10**) or a 4-methylphenyl (**15**) group, activity was lost. Although the amino acid derived region (R^3) has not yet been explored in detail for the imidazole scaffold, inverting the stereochemistry from the natural S- to the unnatural R-configuration led to a 4.7-fold loss of potency and substantially lower efficacy (**2**). Replacement of the leucine – derived isobutyl group with the adamantyl moiety (**16**) led to much lower potency but retention of agonist behavior.

Table 2. SAR of Imidazole-Scaffold Neurotensin-1 Agonists.

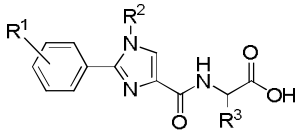

Entry	R^1	R^2	R^3	NTR1 EC_{50} µM	NTR1 E_{max}, %NT
1	2,6-di-OMe	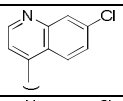		2 - 4	79 - 93
2	2,6-di-OMe	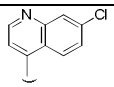		9.4	50
3	2-OMe	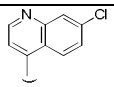		56	100
4	H	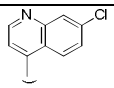		72	100

5	2,6-di-OMe			3.8	59
6	2-OMe			>80	-
7	H			>80	-
8	2,6-di-OMe			66	100
9	2-OMe			>80	-
10	H			>80	-
11	2,4-di-OMe	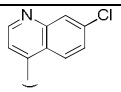		>80	-
12	2,6-di-Cl	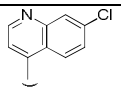		5.2	80
13	2,6-di-Me	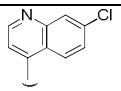		9.2	78
14	2,6-di-OMe			2.3	93
15	2,6-di-OMe	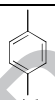		>80	-
16	2,6-di-OMe	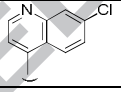		46	100

A high-content imaging assay was used to measure the modulation of the NTR1 receptor in U2OS cells expressing the receptor and a β-arrestin fluorescent reporter. The location of the receptor-arrestin complex was monitored upon receptor activation. The EC_{50} and E_{max} values were calculated relative to the efficacy of the NT peptide at a saturating concentration of 100 nM.

Table 3 shows data for key prior art pyrazole compounds, which were synthesized independently via a solution phase adaptation of the published route[11]. As was observed for the imidazole scaffold, potency declined when the 2,6-dimethoxy case was switched to 2-methoxy (**18**). Two other prior art pyrazoles[7,8] **I-a** (**19**) and **I-b** (**20**) containing the adamantyl moiety and different R^2 groups were purchased and found to be less active as well.

Table 3. SAR of Pyrazole-Scaffold Neurotensin-1 Agonists**.**

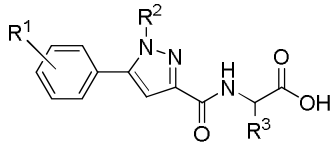

Entry	R^1	R^2	R^3	NTR1 EC_{50} μM	NTR1 E_{max}, %NT
17	2,6-di-OMe	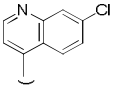		0.75	100
18	2-OMe	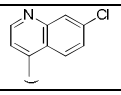		0.97	98

19	2,6-di-OMe	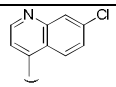		31	100
20	2,6-di-OMe	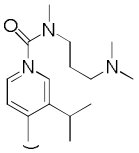		>80	

A high-content imaging assay was used to measure the modulation of the NTR1 receptor in U2OS cells expressing the receptor and a β-arrestin fluorescent reporter. The location of the receptor-arrestin complex was monitored upon receptor activation. The EC_{50} and E_{max} values were calculated relative to the efficacy of the NT peptide at a saturating concentration of 100 nM.

The imidazole **1** and the prior art pyrazole **17** were further profiled in counterassays, and in β-arrestin and Ca^{2+} mobilization assays (**Table 4**). Both compounds were selective for NTR1 over NTR2 and GPR35, but only the imidazole **1** retained activity in the DiscoveRx β-arrestin assay. Consistent with their functioning via the G_q-coupled pathway, both compounds exhibited good functional activity in a Ca mobilization assay, with EC_{50}s at least 5 times better than in the primary NTR1 assay. Additionally, preincubation with the known antagonist **I-b** (IC_{50} = 0.24 nM)[25] inhibited **1** (EC_{100} = 10 μM) mediated NTR1 activation with an IC_{50} of 62 nM, which supports the hypothesis that **1** acts via NTR1 binding (Figure 2).

Table 4. Additional Profiling Assays for Neurotensin-1 Agonists.

Entry	NTR1		NTR2		GPR35		β-arrestin		Ca^{2+} Mobilization	
	EC_{50} μM	E_{max} % NT	EC_{50} μM	E_{max} % NT	EC_{50} μM	E_{max} % NT	EC_{50} μM	E_{max} % NT	EC_{50} μM	E_{max} % NT
1	2.0	79	>80	-	>40	-	6.1	100	0.298	93
17	0.75	100	>80	-	>40	-	>33	-	<0.156	63

A high-content imaging assay was used to measure the modulation of the NTR1, NTR2, and GPR35 receptors in U2OS cells expressing the receptor of interest and a β-arrestin fluorescent reporter. The location of the receptor-arrestin complex was monitored upon receptor activation.
The β-arrestin assay utilizes the DiscoveRx PathHunter system in a CHO-K1 cell line in which the NTR1 receptor is fused in frame with the small enzyme fragment ProLink™ and co-expressed in cells stably expressing a fusion protein of β-Arrestin and the larger, N-terminal deletion mutant of β-gal (called enzyme acceptor or EA). Activation of the GPCR stimulates binding of β-Arrestin to the ProLink-tagged GPCR and forces complementation of the two enzyme fragments, resulting in the formation of an active β-gal enzyme. This interaction leads to an increase in enzyme activity that can be measured using chemiluminescent reagents.
The NTR1 Ca^{2+} Flux assay was performed by ChanTest (Rockville, MD0 and used a CHO cell line which stably expressed the NTR1 receptor.

Overall, it is notable that although the imidazole **1** and the pyrazole **17** possess closely related chemical structures they exhibit substantially different SAR in some respects. First, **1** is less potent (IC_{50}), but similarly efficacious in the NTR1 assay (**Tables 2** and **3**). However, **1** maintained full efficacy in a Ca mobilization assay (**Table 4**), whereas the efficacy of **17** dropped to 63%, consistent with the previously reported[11] value of 54%. Secondly, **1** and **17** gave different responses in the β-arrestin assay (**Table 3**). These differences were deemed important, as identifying a robust full agonist was a key project goal. Thirdly, the two scaffolds apparently respond very differently to structural perturbations. For example, replacing the 7-quinolinyl group with 1-naphthyl reportedly led to potent *antagonist* behavior[11] for the pyrazole **17**. In contrast, identical perturbation of the imidazole scaffold of **1** led to potent and full *agonist* behavior (**14**).

The imidazole **1**, its naphthyl analog **14**, and the pyrazole **17** were advanced to pharmacological screening (**Table 5**). *Overall, despite its structural similarity to the pyrazole **17**, **1** showed substantial advantages on plasma and microsomal stability.* The three compounds exhibited good solubility due to the presence of the carboxylic acid moiety. The PAMPA (**P**arallel **A**rtificial **M**embrane **P**ermeability **A**ssay) assay is used as an *in vitro* model of passive, transcellular permeability. The compounds exhibited overall permeability inversely related to the pH of the donor compartment. Because these NTR1 agonists are envisioned as predecessors of psychoactive drugs, a preliminary assessment of their potential to cross the blood brain barrier (BBB) was performed. When incubated with an artificial membrane that models the BBB, much lower permeability was observed in contrast to our recently reported **ML314**

which gave P_e 399 cm/s in the same assay.[14] The imidazoles **1** and **14** were 4 times less permeable than **17**. These observations are consistent with the carboxylic acid function in the compounds, and may present an opportunity for future enhancements. Compounds **1** and **14** exhibited substantial plasma protein binding, but lower than that of **17**. Importantly, the unbound fraction for **1** and **14** was about five to ten times greater than for **17**. The differences observed for **1** and **14** when compared to **17** in the BBB and protein binding models may be due in part to zwitterionic character associated with the imidazoles. The imidazole **1** also showed excellent stability in plasma, significantly better than that of either **14** or **17**. Additionally, **1** showed excellent stability in human and modest stability in mouse liver homogenates, in contrast to the pyrazole **17** which gave values of 76% and 46% in the same assays run in triplicate. None of the compounds showed toxicity (>50 μM) toward human hepatocytes after 24 hours.

Table 5. Summary of in vitro ADME/T Properties of NTR1 Agonists.

ADME/T Assay Panel Component		1	14	17
Aqueous Solubility in pION's buffer (μg/mL) *[μM]*[a] pH 5.0/6.2/7.4		>52 / >52 / >52 *[>99 / >99 / >99]*	102.6 / >145 / >145 *[247 / >297 / >297]*	52.9 / >155 / >155 *[113 / >296 / >296]*
PAMPA Permeability, P_e ($x10^{-6}$ cm/s) Donor pH: 5.0 / 6.2 / 7.4 Acceptor pH: 7.4		363 / 17 / 6	953 / 145 / 12	1267 / 725 / 70
BBB-PAMPA Permeability, Pe ($x10^{-6}$ cm/s) Donor pH: 7.4 Acceptor pH: 7.4		1.2	1.1	4.8
Plasma Protein Binding (% Bound)	Human 1 μM / 10 μM	98.7 / 98.7	97.9 / 98.0	99.6 / 99.7
	Mouse 1 μM / 10 μM	92.2 / 91.4	96.4 / 95.4	96.6 / 97.1
Plasma Stability (%Remaining at 3 hrs) Human/Mouse		100 / 100	76.0 / 76.0	88.9 / 70.7
Hepatic Microsome Stability (% Remaining at 1hr) Human/Mouse		100 / 59	100 / 76	76 / 46
Toxicity Towards Fa2N-4 Immortalized Human Hepatocytes LC_{50} (μM), after 24 hours.		>50	>50	>50

[a] Solubility also expressed in molar units (μM) as indicated in *italicized [bracketed values],* in addition to μg/mL units.

To assess the potential for promiscuous activity across a range of GPCRs, **1** and **17** were submitted to the Psychoactive Drug Screening Program (PDSP) at the University of North Carolina (Bryan Roth, PI)[26]. The results (**Figure 1**) indicate **1** shows very little potential for promiscuity across a range of GPCRs at 10 μM concentration. Contrarily, the pyrazole **17** showed a somewhat higher potential for promiscuity. Follow up dose response studies revealed K_i values of >10 μM (DAT) and 10 μM (NTS1) for **1**, and >10 μM (DAT), 5.2 μM (DOR), 3.4 μM (MOR), and 3.3 μM (NTS1) for **17**. It is not known whether these activities in binding assays are translated into functional modification of the activities of these receptors.

In summary, the imidazole **1** was designed via a scaffold hop approach based on the previously disclosed pyrazole **17**, which was designed in part from knowledge of SR48692 (**I-a**, **Table 1**). Taken together, these advances underscore the value of drug design via iterative / intuitive structural enhancement of an identified scaffold. Despite having substantial structural similarity to the pyrazole **17**, the imidazole **1** exhibits intriguing differences / advantages in chemical and biological properties. Although **1** is less potent than **17** and comparably potent to **14**, it is a more effective agonist than **17** in the calcium mobilization assay. Identification of a full agonist was a primary objective for this program. The imidazole **1** also showed a much better pharmacology profile, including lower protein binding along with improved plasma and hepatic microsomal stability. These improvements may enable **1** or future analogs of it to achieve a distribution profile more favorably disposed toward *in vivo* activity. Compound **1** also showed minimal promiscuity. As it is tractable from a synthetic chemistry perspective and appears more tolerant of variation at the R^2 position, it represents a strong platform on which to launch a medicinal chemistry-based program for further enhancement.

Acknowledgements

This work was supported by NIH grants 1 R03 MH089653-01 to LSB and an NIH Molecular Libraries grant (U54 HG005033-03) to the Conrad Prebys Center for Chemical Genomics at the Sanford Burnham Medical Research Institute, one of the comprehensive centers of the NIH Molecular Libraries Probe Production Centers Network (MLPCN).

References and notes

1. Results from the 2011 National Survey on Drug Use and Health: Summary of National Findings; NSDUH Series H-44, HHS Publication No. (SMA) 12-4713. Substance Abuse and Mental Health Services Administration: Rockville, MD, 2012. http://www.samhsa.gov/data/NSDUH/2011SummNatFindDetTables/ Index.aspx (accessed September 3, 2013).
2. Caraway, R.; Leeman, S. E. *J. Biol. Chem*. **1973**, *248*, 6854.
3. Quirion, R.; Rowe, W. B.; Lapchak, P. A.; Araujo, D. M.; Beaudet, A. *Ann. N.Y. Acad. Sci*. **1992**, *668*, 109.
4. Sarret, P.; Perron, A.; Stroh, T.; Beaudet, A. *J. Comp. Neurol*. **2003**, *461*, 520.
5. Uhl, G. R. Ann. N.Y. Acad. Sci. **1982**, *400*, 132.
6. Walker, N.; Lepee-Lorgeoux, I.; Fournier, J.; Betancur, C.; Rostene, W.; Ferrara, P.; Caput, D. *Brain Res. Mol. Brain Res*. **1998**, *57*, 193.
7. Gully, D.; Labeeuw, B.; Boigegraiin, R.; Oury-Donat, F.; Bachy, A.; Poncelet, M.; Steinberg, R.; Suaud-Chagny, M.F.; Santucci, V.; Vita, N.; Pecceu, F.; Labbe-Jullio, C.; Kitabgi, P.; Soubrie, P.; Le Fur, G.; and Maffrand, J.P. *J. Pharmacol. Exper. Therapeut.* **1997**, *280*, 802.
8. Gully, D.; Canton, M.; Boigegraiin, R.; Jeanjean, F.; Molimard, J-C.; Poncelet, M.; Gueudet, C.; Heaulme, M.; Leyris, R.; Brouard, A.; Pelaprat, D.; Labbe-Jullio, C.; Mazellai, J.; Soubrie, P.; Rostene, W.; Kitabgi, P.; and Le Fur, G. *Proc. Natl. Acad. Sci. USA*. **1993**, *90*:65.
9. Hanson, G.R.; Hoonakker, A.J.; Alburges, M.E.; McFadden, L.M.; Robson, C.M.; Frankel, PS. *Neuroscience* **2012**, *203*, 99.
10. Myers, R.M.; Shearman, J.W.; Kitching, M.O.; Ramos-Montoya, A.; Neal, D.E.; and Ley, S.V. *ACS Chem. Bio*. **2009**, *4*(*7*), 503.
11. Thomas, J.B.; Navarro, H.; Warner, K.R.; and Gilmour, B. *Bioorg. Med. Chem. Lett*. **2009**, *19*, 1438.
12. Thomas, J.B. and Runyon, S.P. WO 2011/156557 A2, **2011**.
13. Fan, Y.; Lai, M.H.; Sullivan, K.; Popiolek, M.; Andree, T.H.; Dollings, P.; and Pausch, M.H. *Bioorg. Med. Chem. Lett*. **2008**, *18*, 5789.
14. Peddibhotla, S; Hedrick, M.P.; Hershberger, P.; Maloney, P.R.; Li, Y.; Milewski, M.; Gosalia, P.; Gray, W.; Mehta, A.; Sugarman, E.; Hood, B.; Suyama, E.; Nguyen, K.; Heynen-Genel, S.; Vasile, S.; Salaniwal, S.; Stonich, D.; Su, Y.; Mangravita-Novo, A.; Vicchiarelli, M.; Roth, G.P.; Smith, L.H.; Chung, T.D.Y.; Hanson, G.R.; Thomas, J.B.; Caron, M.G.; Barak, L.S. and Pinkerton, A.B. *ACS Med. Chem Lett*. **2013**, *4*, 846.
15. Lange, J.H.; van Stuivenberg, H.H.; Coolen, H.K.A.C; Adolfs, T.J.P.; McCreary, A.C.; Keizer, H.G.; Wals, H.C.; Veerman, W.; Borst, A.J.M.; de Looff, W.; Verveer, P.C. and Kruse, C.G. *J. Med. Chem*. **2005**, *48*, 1823.
16. Singh, B. and Collins, J.C. *J. Chem. Soc. Chem. Comm*. **1971**, 498.
17. Weintraub, L.; Oles, S.R. and Kalish, N. *J. Org., Chem.* **1968**, *33*(*4*), 1679.
18. Smith, R.A.; Fathi, Z.; Achebe, F.; Akuche, C.; Brown, S.E.; Choi, S.; Fan, J.; Jenkins, S.; Kluender, H.C.E.; Konkar, A.; Lavoie, R.; Mays, R.; Natoli, J.; O'Connor, S.J.; Ortiz, A.A.; Su, N.; Taing, C.; Tomlinson, S.; Tritto, T.; Wang, G.; Wirtz, S.N.; Wong, W.; Yand, X.F.; Ying, S.; and Zhang, Z. *Bioorg. Med. Chem. Lett*. **2007**, *17*, 2706.
19. Ogonor, J.I. *Tetrahedron* **1981**, *37*(*16*), 2909.
20. McCarthy, J.R.; Wright, D.L.; Schuster, A.J.; Abdallah, A.H.; Shea, P.J. and Eyster, R. *J. Med. Chem*. **1985**, *28*, 1721.
21. Zhu, C.; Hansen, A.R.; Bateman, T.; Chen, Z.; Holt, T.G.; Hubert, J.A.; Karanam, B.V.; Lee, S.J.; Pan, J.; Qian, S.; Reddy, V.B.G.; Reitman, M.L.; Strack, A.M.; Tong, V.; Weingarth, D.T.; Wolff, M.S.; MacNeil, D.J.; Weber, A.E.; Duffy, J.L. and Edmondson, S.D. *Bioorg. Med. Chem. Lett*. **2008**, *18*, 4393.
22. Asproni, B.; Pau, A.; Bitti, M.; Melosu, M.; Cerri, R.; Dazzi, L.; Seu, E.; Maciocco, E.; Sanna, E.; Busonero, F.; Talani, G.; Pusceddu, L.; Altomare, C.; Trapani, G. and Biggio, G. *J. Med. Chem.* **2002**, *45*, 4655.
23. Khanna, I.K.; Weier, R.M.; Yu, Y.; Xu, X.D.; Koszyk, F.J.; Collins, P.W.; Koboldt, C.M.; Veenhuizen, A.W.; Perkins, W.E.; Casler, J.J.; Masferrer, J.L.; Zhang, Y.Y.; Gregory, S.A.; Seibert, K. and Isakson, P.C. *J. Med., Chem.* **1997**, *40*, 1634.
24. Adams, R.S.; Duffey, M.; Gould, A.E.; Greenspan, P.D.; Kulkarni, B.A. and Vos, T.J. US 2008/0171754, **2008**.

25. Schaffer, P.; Laplace, M.C.; Bernat, A.; Prabonnaud, V.; Gully, D.; Lespy, L. and Herbert, J.M. *J. Cardiovasc. Pharmacol*. **1998**, *31*, 545.
26. NIMH Psychoactive Drug Screening Program, http://pdsp.med.unc.edu/indexR.html.

Scheme 1, Preferred route: Synthesis of **1,** conditions: a.[24] 1. NaOAc, water, 1,1-dibromo-3,3,3-trifluoroacetone, 100 °C, 30 min. 2. 2,6-dimethoxybenzaldehyde, ammonium hydroxide, water, methanol, 52%; b.[24] NaOH, water, 100 °C, 94%; c. $SOCl_2$, EtOH, 75 °C; d. 7-chloro-4-iodoquinoline, cesium carbonate, butyronitrile, 110 °C, 20 h, 43%; e. KOH, EtOH, water; f. L-leucine t-butyl ester, EDC, HOBt, triethylamine, DMF, 83%; g. trifluoroacetic acid, DCM, reverse phase HPLC purification, 82%.

Scheme 1, Alternate route: Synthesis of **1,** conditions: h. 7-chloro-4-aminoquinoline, EtMgBr, diethyl ether, tetrahydrofuran, 75 °C, 9%; i. 1. Ethyl bromopyruvate, sodium bicarbonate, EtOH, reflux, 22 h, work up. 2. pTsOH, toluene, reflux, 4 h, 17%.

Figure 1. Comparison of **1** and **17** in a GPCR panel of assays (% inhibition at 10 μM).

Figure 2. Inhibitory dose response of NTR1 antagonist **I-b** (SR142948A) in the presence of agonists **1** (10 μM) and NT(8-13) (5 nM).

Scheme 1

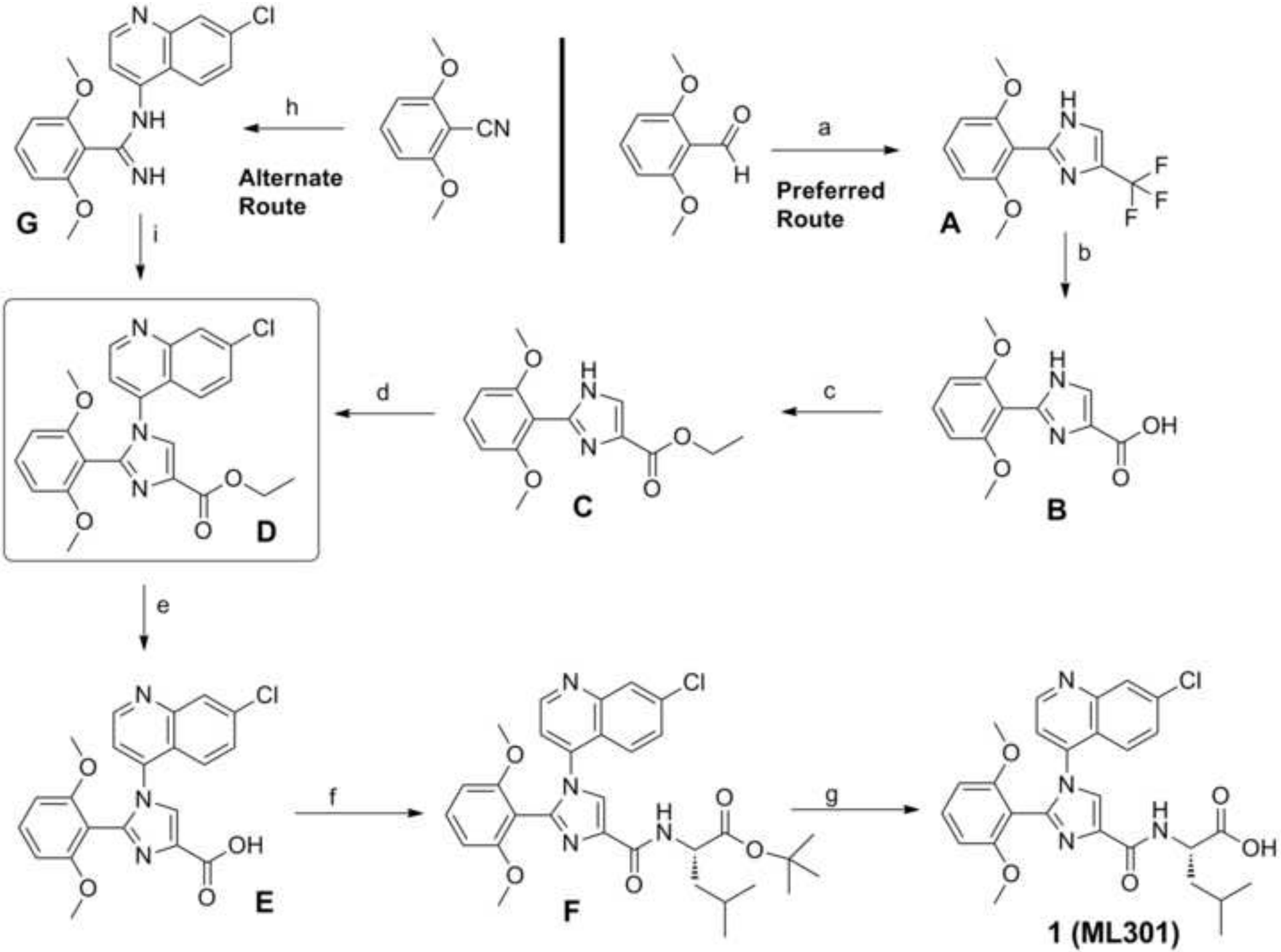

Figure 1

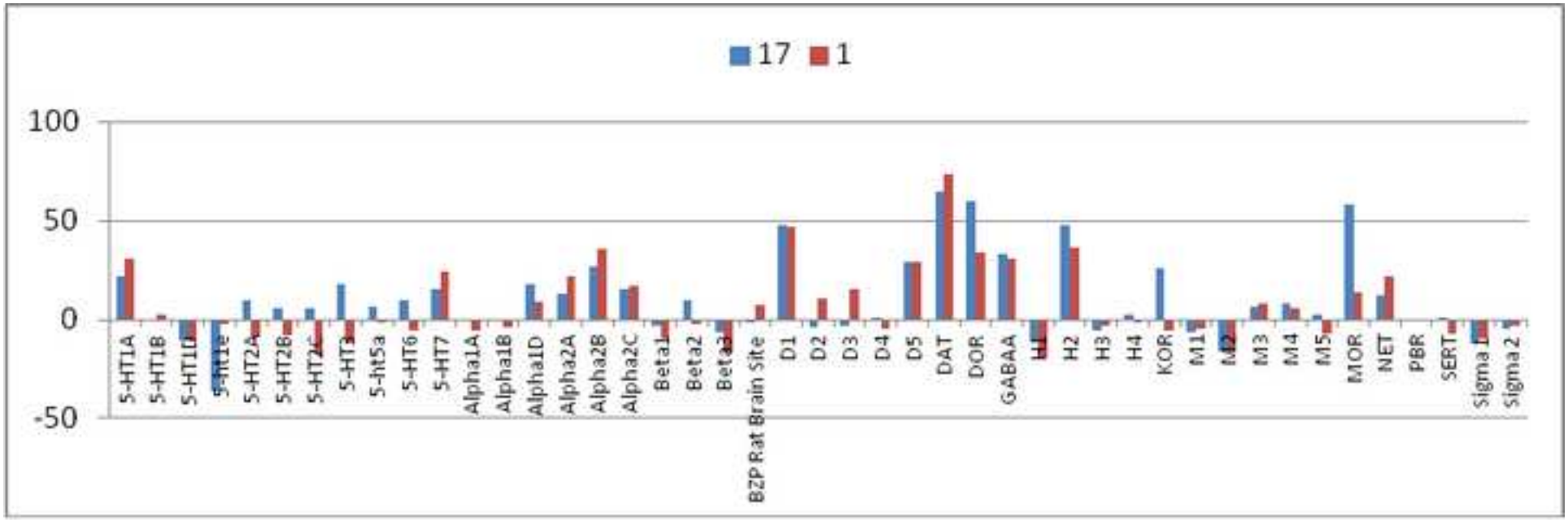

Figure 2

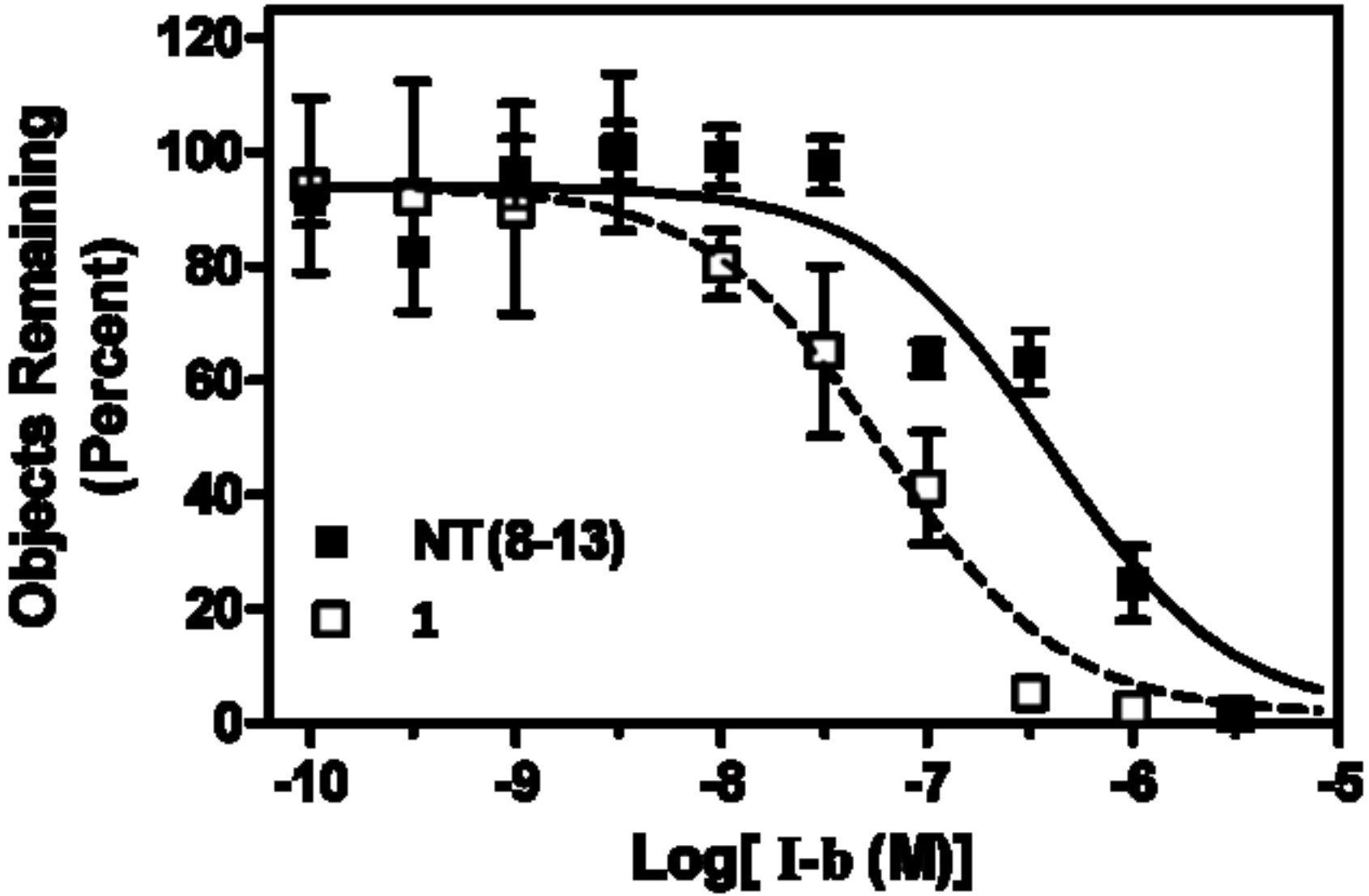

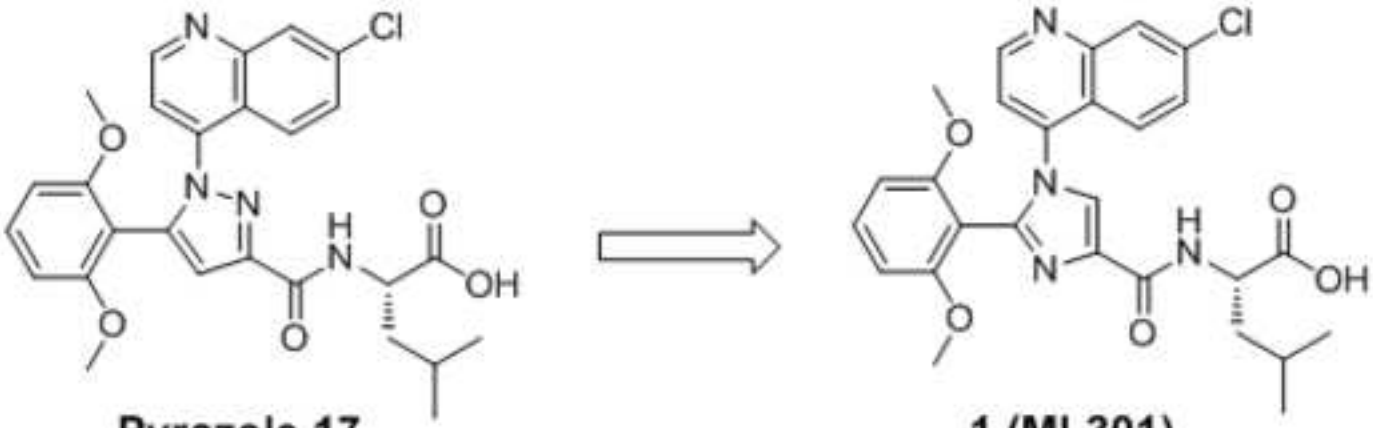

Pyrazole 17 1 (ML301)

Compound	NTR1		NTR2		β-arrestin		Ca^{2+} Mobilization	
	EC_{50} μM	E_{max} % NT	EC_{50} μM	E_{max} % NT	EC_{50} μM	E_{max} % NT	EC_{50} μM	E_{max} % NT
1	2.0	79.39	>80	-	6.1	100	0.298	93
17	0.75	100	>80	-	>33	-	<0.156	63